ELSEVIER

Catalysis Today 70 (2001) 341–357

CATALYSIS TODAY

www.elsevier.com/locate/cattod

Chaos and synchronisation in heterogeneous catalytic systems: CO oxidation over Pd zeolite catalysts

M.M. Slinko [a], A.A. Ukharskii [a], N.V. Peskov [b], N.I. Jaeger [c,*,1]

[a] *Institute of Chemical Physics, Russian Academy of Science, Kosygina Str. 4, 117334 Moscow, Russia*
[b] *Department of Computational Mathematics and Cybernetics, Moscow State University, 119899 Moscow, Russia*
[c] *Institut für Angewandte und Physikalische Chemie, FB 2, Universität Bremen, PF 330440, 28334 Bremen, Germany*

Abstract

The influence of experimental parameters on the structure of global reaction rate oscillations and the coupling of local oscillators on a catalyst bed in a continuous stirred tank reactor is studied for the oxidation of CO on zeolite supported palladium catalysts. Global coupling can be achieved via mass transfer through the gas phase or via heat transfer in the case of a support of high heat conductivity. Characteristic differences in the activity of catalysts as well as in the period and the amplitude of the oscillations are related to the size of the palladium clusters and can be simulated by adding the state of the oxidation of the metal surface as a parameter to a common kinetic model. The analysis of observed chaotic behaviour leads to the conclusion that diffusional chaos characteristic of a distributed system is observed on the level of the zeolite crystallite that supports the palladium clusters.

Keywords: CO oxidation; Pd supported catalyst; Kinetic oscillations; Coupled oscillators; Chaotic oscillations

1. Introduction

Heterogeneous catalytic reactions are highly nonlinear systems usually operated under conditions far from thermodynamic equilibrium where temporal and spatiotemporal organisation become possible. The very rich dynamic behaviour observed in many heterogeneous catalytic systems includes regular periodic, quasiperiodic and mixed mode oscillations as well as deterministic chaos. Analysis and simulation of the experimental observations have led to a detailed understanding of the underlying reaction mechanisms in the past decades especially due to the direct observation of catalytic surfaces under high vacuum conditions with the help of surface science methods [1–3].

Oscillatory behaviour can arise on various levels of a heterogeneous catalytic system. The first level would be an element on a single crystal surface with oscillatory behaviour which can be described by a kinetic point model. The second level is represented by a spatially extended single crystal surface commonly including spatial inhomogeneities or by a single metal cluster bounded by differently indexed planes. The third level for massive catalysts may be considered as a whole polycrystalline metallic surface and for supported catalysts as a pellet. Finally, the fourth level for supported catalysts is represented by a catalyst bed. From the second level up always an array of oscillators has to be considered and the observed more or less synchronised behaviour not only depends upon the properties of local oscillators but also on the strength and the nature of the coupling between them [2]. The

* Corresponding author.
E-mail addresses: slinko@polymer.chph.msk.ru (M.M. Slinko), peskov@cs.msu.su (N.V. Peskov), jse@uni-bremen.de (N.I. Jaeger).
[1] Co-corresponding author.

0920-5861/01/$ – see front matter
PII: S0920-5861(01)00342-X

observation of periodic oscillatory behaviour of the global reaction rate means complete synchronisation of local oscillators on each level of a heterogeneous catalytic system. Coupling between local oscillators may occur via surface diffusion, diffusion through the gas phase and heat transfer. The dominant mechanism of synchronisation will depend upon the nature of the local oscillator and the conditions of the experiment. In single crystal UHV studies surface and gas phase diffusion are the main mechanisms of coupling, while at atmospheric pressure in the case of supported catalysts heat transfer may also be important for the synchronisation of oscillations, especially in the case of highly exothermic reactions.

Gas phase coupling operates through the variation of reactant concentrations in a reactor due to reaction rate oscillations. In the case of a continuous stirred tank reactor (CSTR) concentration changes in the gas phase due to local changes in reaction rate are felt on the entire catalyst surface simultaneously and practically without delay on the time scale of the oscillations; thus this coupling is global. Surface diffusion and heat transfer are coupling mechanisms which operate on smaller length scales and may be only nearest neighbours communicate with each other. The effect dies out with increasing distance and hence these mechanisms of coupling are considered to be nonlocal (short range) or even local.

The verification of the dominant mechanism of synchronisation can be difficult even in the case of single crystal studies under UHV conditions, where the heat produced by the reaction is too small and only coupling via surface diffusion and via the gas phase is relevant. Forcing experiments and the examination of spatial surface structures demonstrated that coupling by surface diffusion dominates during CO oxidation on Pt(1 0 0), while gas phase coupling is the main mechanism of synchronisation for the same reaction on a Pt(1 1 0) single crystal surface [4,5].

It is more difficult to establish the prevailing mechanism of synchronisation in high pressure experiments, where all three mechanisms of coupling can operate. Tsai et al. [6] established mass transport through the gas phase as the mechanism responsible for the synchronisation in the case of the oscillatory CO oxidation on a polycrystalline Pt surface. However, the role of coupling via heat transfer was not evaluated. Onken and Wolf [7] studied the oxidation of ethylene on two active Pt/SiO_2 areas embedded at a distance into a wafer of inactive silica. They identified heat transfer through the wafer as the dominant mechanism of synchronisation on the level of a catalyst bed. In this work, on the other hand, gas phase coupling was not eliminated and its role was not analysed.

The lack of synchronisation may lead to the appearance of complicated time series of the global reaction rate, which are frequently observed in heterogeneous catalytic systems. In this case it has to be determined whether the complicated oscillations arise due to the superposition of frequencies of local oscillators or the observed complicated dynamic behaviour reveals all the properties of deterministic chaos. Chaotic behaviour can originate on various levels of a heterogeneous catalytic system [2,8]. It can be temporal (low dimensional) chaos, which describes the dynamic behaviour of one oscillator or spatiotemporal (high dimensional) chaos, which arises in an array of coupled oscillators [9]. The first type of chaos can be simulated with point or lumped models, representing ordinary differential equations, while for the description of chaotic behaviour in distributed systems partial differential equations or systems of coupled maps are used.

In low pressure single crystal studies deterministic chaos has been identified for three systems: $CO + O_2/Pt(1\,1\,0)$ [10], $NO + H_2/Pt(1\,0\,0)$ [11] and $CO + NO/Pt(1\,0\,0)$ [12]. In all these systems chaotic dynamics was observed in a very narrow region of experimental parameters. The best characterised of these systems is the CO oxidation over Pt(1 1 0) single crystal surface, where low-dimensional chaos with an embedding dimension of five was determined [10].

In high pressure studies the chaotic behaviour has been identified for massive metallic [13] and supported catalysts [14]. In these systems chaotic oscillations are observed in a much larger region of temperature and reactant pressure. This fact may indicate that on the highest levels of heterogeneous catalytic systems the observed complicated dynamic behaviour may not be inherent in the point model, which describes the system as one homogeneous local oscillator, but rather results from the coupling of an array of different local oscillators.

The oxidation of CO over Pd zeolite catalysts displays extremely rich dynamic behaviour including regular periodic, self-similar mixed mode and chaotic oscillations [15,16]. In the case of zeolite catalysts

the reaction proceeds on the active metal particles with a narrow size distribution embedded within the zeolite matrix. The coupling of distant Pd clusters via diffusion on the surface of the zeolite support can be neglected due to very small values of surface diffusion coefficients and gas phase synchronisation prevails with coefficients of diffusion in the order of 10^{-4}–10^{-5} cm^2/s in the channels of the zeolite for the reacting molecules. Therefore at least one of the mechanisms of coupling can be excluded on the level of a zeolite crystallite and the reaction is considered to be a suitable model systems for the study of synchronous and chaotic behaviour.

It is the goal of the present work to analyse the conditions for the appearance and the properties of regular and chaotic oscillations. Special attention is paid to the effect of the size of the embedded Pd clusters on the dynamic behaviour of the system. The possible dominant mechanisms of the coupling of local oscillators on the level of the catalyst bed in a CSTR will be established.

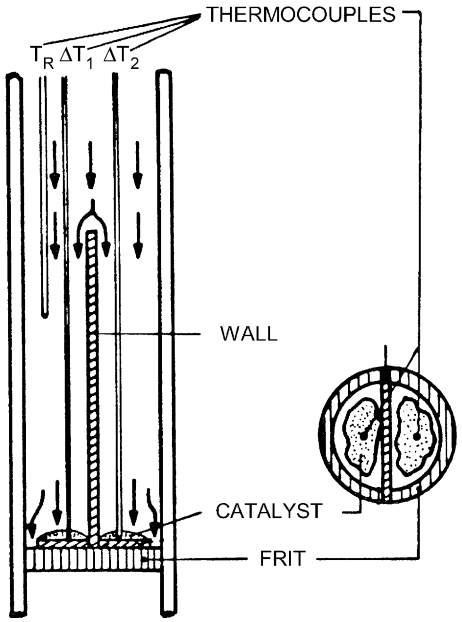

Fig. 1. Reactor used in the study, allowing the partition of the reactor volume between two parts of the catalyst layer with different properties of the oscillations (from Ref. [24] reproduced by permission of the Royal Society of Chemistry).

2. Experimental

Experiments were carried out in a continuous flow glass reactor under atmospheric pressure [16]. A certified mixture of CO and N_2 (10 vol.% CO, 99.97% pure Messer-Griesheim, in N_2) was passed through a glass tube with quartz pellets held at 500 K to remove traces of volatile metal carbonyls and then mixed with oxygen (99.995% pure, Messer-Griesheim). Nitrogen (99.995% pure, Messer-Griesheim) was added as a balance.

The reaction mixture was fed into the reactor with a flow rate of 150 cm^3/min corresponding to a linear flow velocity of 1.89 cm/s. The flow rates were controlled by thermal mass flow controllers (HI-TEC, 1% precision). The gas composition was changed by varying the CO concentration up to 3.5 vol.%. The outlet CO, CO_2 concentrations were measured by IR analyser URAS 10 E.

The catalyst was applied under shallow bed conditions on a glass frit in the reactor depicted in Fig. 1. The calculations of a small axial Peclet number and the characteristics of residence time spectra indicate that for the given experimental conditions, the behaviour of the flow reactor is similar to a CSTR. For the study of the coupling of two different Pd zeolite catalysts a Teflon partition can be inserted into the reactor to prevent the gas phase coupling between two individual parts of the catalyst layer. Fig. 1 shows the reactor with partition. The dynamic behaviour of individual parts of the catalyst bed was monitored by two sensitive thermocouples positioned on top of the surface of the catalyst. Each thermocouple gives a measure of the heat production due to the reaction rate on the catalyst in the vicinity of its spotweld.

A NaX faujasite (Si/Al = 1.25) was used as a matrix. $[Pd(NH_3)_4]^{2+}$ cations were introduced into the faujasite cavities by ion exchange overnight at room temperature from solutions of the corresponding chloride [18]. The supporting zeolite crystallites had an average size of 5 μm in diameter. The Pd loading was 0.05 and 0.01 wt.%. A palladium content of 0.05 wt.% corresponds to about one Pd atom per 10 unit cells. The metal phase was precipitated by an autoreduction process during the temperature programmed decomposition of the ammine complex or alternatively by calcination of the sample followed by reduction

Table 1
Pd zeolite catalysts used in the present study

Catalyst	Pd loading (wt.%)	Pd surface area (cm^2)	Amount of catalyst (mg)	Size of Pd crystallites (nm)
A	0.05	15.1	60.4	10
B	0.05	15.1	24.2	4
C	0.01	5	100	10
D	0.01	5	40	4

with hydrogen yielding narrow particle size distribution around 10 and 4 nm, respectively [18]. Metal clusters of a size exceeding the dimension of the supercage by far can be grown within the faujasite host by local destruction of the surrounding matrix [19]. The samples were investigated with a Philips EM 420 electron microscope operated at 120 kV. Compositions and notations of samples are listed in Table 1. Prior to each experimental run the catalyst was oxidised for 12 h in flowing synthetic air at 633 K. The amount of the catalyst was chosen such that the Pd surface area was the same for both catalysts.

3. Results

3.1. Particle size effect

The effect of the size of the palladium crystallites on the activity and the dynamic behaviour of the catalysts has been studied under similar experimental conditions in the reactor, shown in Fig. 1 but without partition. The activity and the dynamic behaviour of the system have been analysed under similar experimental conditions for catalysts with the same Pd loading but different size of the Pd particles. Fig. 2 depicts the dependence of the reaction rate upon the CO concentration in the reactor and the regions and amplitudes of the reaction rate oscillations for catalysts A and B for the same palladium surface area of 15.1 cm^2 (Table 1). The measurement of the curves for increasing (open triangles) and decreasing CO concentration (open circles) reveal an hysteresis phenomenon. However, no true hysteresis has been established since the differences in the kinetic curves arise due to enhanced reduction of the oxidised Pd particles at high CO concentrations. As a result the initial kinetic curve obtained over the pre-oxidised catalyst could not be reproduced in the second cycle.

Fig. 2 depicts the region of oscillations for both catalysts. The effective CO concentration in the reactor is used as the abscissa, which under appropriate conditions can oscillate in time. Therefore, the amplitudes of oscillations are shown as slanted bars which indicate the maximum and the minimum of oscillations. The CO inlet concentration can be derived from the figure by adding the CO_2 concentration in the effluent (ordinate) to the effective CO concentration plotted on the abscissa.

Fig. 2 shows that the difference between the two branches is much larger in the case of catalyst B with the smaller Pd particles (4 nm) and that the reaction rate on the reduced catalyst is considerably enhanced compared to the initially oxidised catalyst. Moreover, the activity of catalyst B is higher, the region of oscillations more extended and the amplitudes larger compared to catalyst A loaded with 10 nm Pd particles. Similar results have been obtained for catalysts C and D with 0.01 wt.% Pd although the differences in the activity were less pronounced.

Significant differences in the oscillatory behaviour were also found in dependence on the particle size under the same experimental conditions. While for a low CO inlet concentration (0.3 vol.%) regular periodic oscillations could be established in the case catalyst A with 10 nm Pd this was not possible for catalyst B containing 4 nm particles. In the latter case, the oscillations are irregular and it was not possible to find experimental conditions (temperature, CO inlet concentration), where regular periodic oscillations could be observed.

Even more pronounced differences in the oscillatory behaviour of catalysts A and B are shown in Fig. 3 for higher inlet CO concentration equal to 0.5 vol.%. Catalyst B with 4 nm Pd particles was found to be more active and to spend longer time in the high activity state compared to catalyst A with higher frequency oscillations.

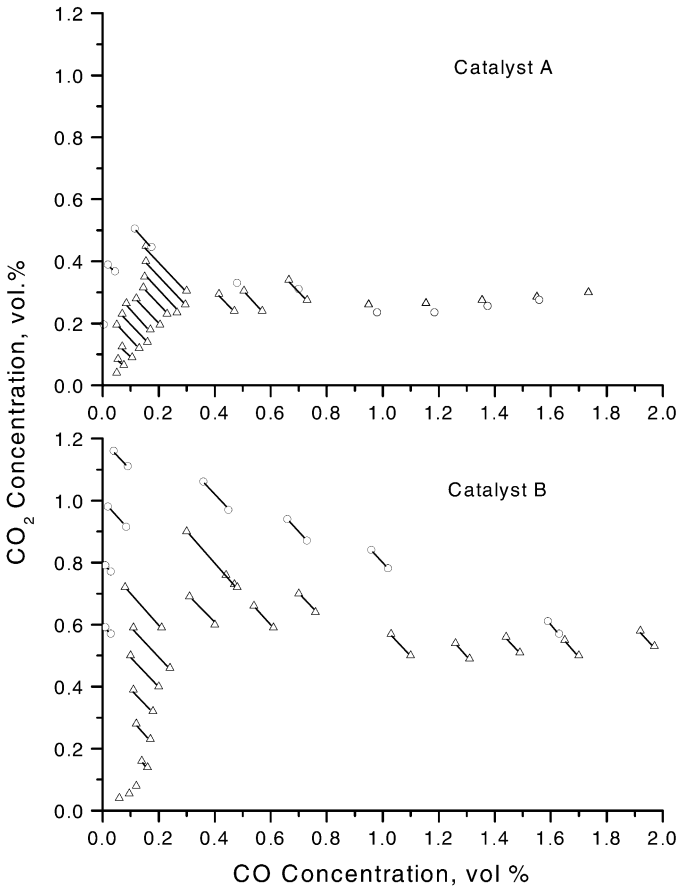

Fig. 2. Ascending (△) and descending (○) branches of the reaction rate as a function of CO concentration in the feed for catalysts A and B at 503 K. The region of kinetic oscillations is indicated by slanted lines which represent the amplitudes of the oscillations.

3.1.1. Synchronised behaviour

Regular periodic oscillations have been obtained over catalyst A at 503 K in a very narrow region of CO inlet concentrations between 0.3 and 0.34 vol.% in the case of the pre-oxidised catalyst. At lower temperatures the reaction proceeded in a steady state. Fig. 4 shows for a time span of 8 h how amplitude, period and activity increase with time on stream and the wave form slowly changes. Initially, the pre-oxidised catalyst A displayed very low activity and it took some time for the appearance of oscillations. The observed changes are attributed to the establishment of a more reduced state of the catalyst. Compared to the experimental conditions depicted in Fig. 2, the reduction process is very slow at low CO concentrations. With increasing activity of the catalyst the system spends more time in the high activity state and the wave form tends to approach that of a catalyst exposed to higher CO concentrations prior to the experiment (see Fig. 4). Fig. 5 demonstrates the different shapes of oscillations at a CO concentration of 0.3% following the pre-treatment of the catalyst by oxygen and by a reaction mixture containing 1% of CO. In the case of the more reduced catalyst, the period of the oscillations has increased and the system spends longer time in the high activity state.

3.1.2. Transition to chaos

Regular oscillations over catalyst A can keep their periodicity as long as 17 h. The complication of the

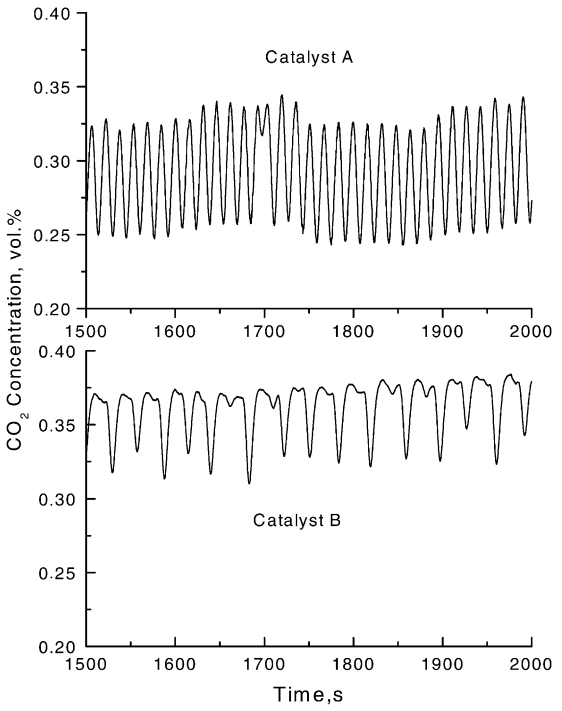

Fig. 3. The difference in the oscillatory behaviour for catalysts with different sizes of Pd clusters at 503 K and 0.5% CO inlet concentration (from Ref. [24] reproduced by permission of the Royal Society of Chemistry).

dynamic behaviour has been detected following a slow increase of the CO inlet concentration in very small steps (0.02–0.04%). Fig. 6 demonstrates that the system undergoes a sequence of transitions from regular to more complex temporal behaviour. The regular oscillations start to destabilise at $C_{CO} = 0.34\%$, when the periodic state seems to be randomly disrupted by short perturbations. It can be seen that with increasing CO concentration the irregular perturbations become more and more frequent until fully developed aperiodic behaviour is eventually reached at 0.4% CO.

The calculations of the largest Lyapunov exponent λ by the Rosenstein method [20] for the time series, corresponding to 0.4% CO yield a value $\lambda = 0.08$ bit/s. The positive value of λ indicates an exponential divergence of nearby trajectories on the attractor, which is the main characteristic of chaos. No signs of the destruction of a torus or of the period doubling scenario can be detected by visual inspection of the time series, presented in Fig. 6. This suggests intermittency as a candidate for the route to chaos. The intermittency scenario is characterised by the existence of regular (laminar) phases along the evolution of a system variable interrupted by bursts (or perturbations) of irregular behaviour [21]. The detailed study of

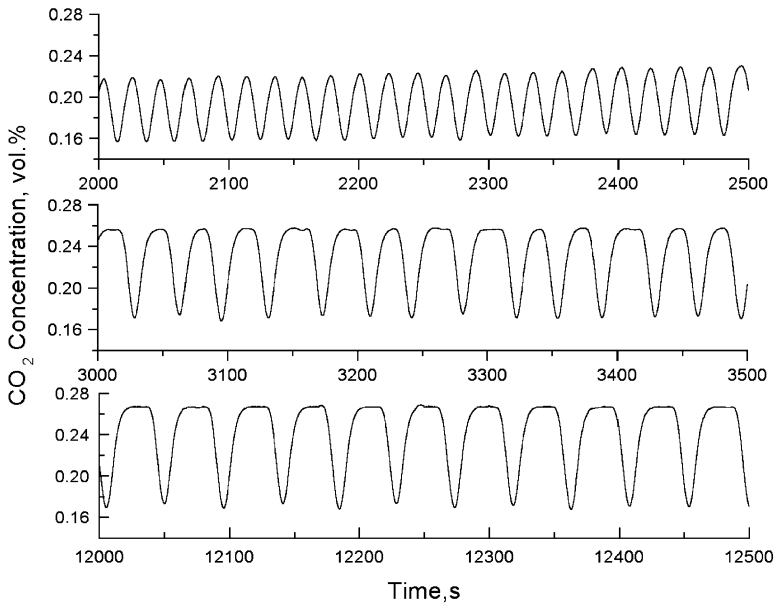

Fig. 4. The evolution of regular oscillations over catalyst A with time at 503 K and 0.3% CO inlet concentration.

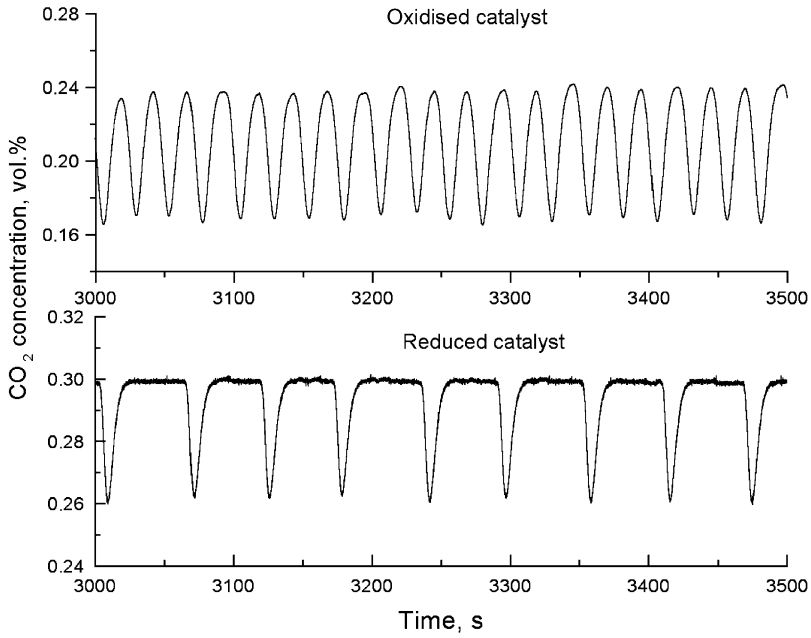

Fig. 5. Different waveform of oscillations obtained following the pre-treatment of the catalyst: (a) pre-oxidised catalyst; (b) oxidised catalyst followed by reduction in a reactant mixture containing 1% CO for 30 min.

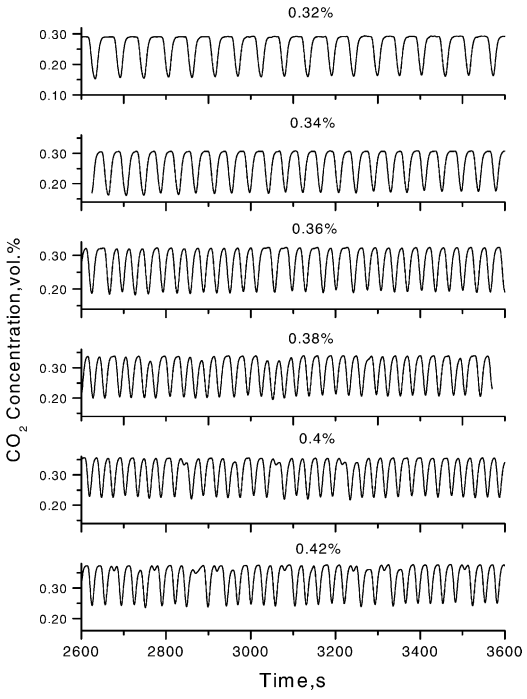

Fig. 6. Increasing complexity of the reaction rate oscillations observed in the case of catalyst A for increasing CO concentration.

the developed chaotic behaviour and the identification of the route to chaos is presented in Ref. [22].

3.1.3. Chaotic behaviour

For high CO concentrations a very complicated dynamic behaviour has been observed over both catalysts A and B and the time series at inlet CO concentration equal to 1.1% are shown in Fig. 7a. Fig. 7b depicts the corresponding Fourier power spectra. Catalyst B with 4 nm Pd particles again shows the higher activity. At the minimum of the amplitude of the oscillations the reaction rate over this catalyst is even larger than the maximum reaction rate over catalyst A containing the larger Pd particles. For both time series, the Fourier power spectra display the shape of a broadband peak, which is one of the main characteristics for chaotic systems. The larger amplitudes of the oscillations and the more significant contribution of lower frequencies in the case of catalyst A clearly show up in the spectra.

The experimental data shown in Fig. 7a represent single-variable time series of the CO_2 concentration $s_k = s(k\Delta t)$, where $k = 0, 1, 2, \ldots, N$, and N is the number of points separated by the same time step Δt equal to 0.1 s. From the scalar time series, it is possible

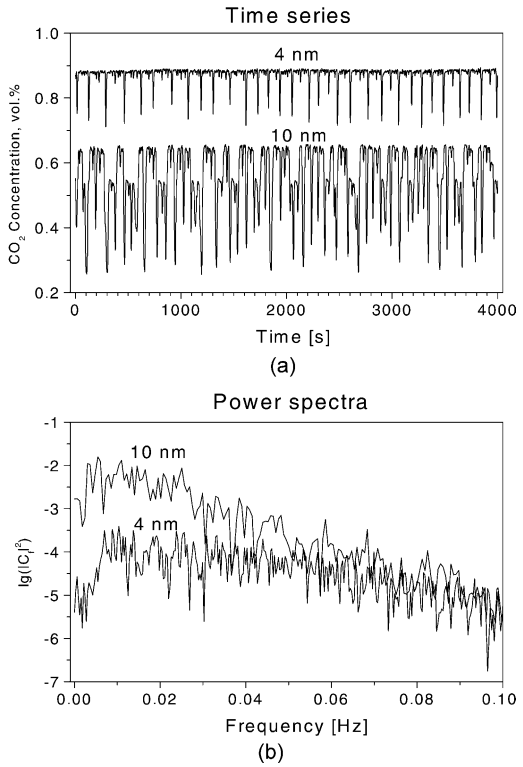

Fig. 7. (a) Chaotic time series observed over catalysts A and B at 503 K and 1.1% CO inlet concentration; (b) corresponding Fourier power spectra.

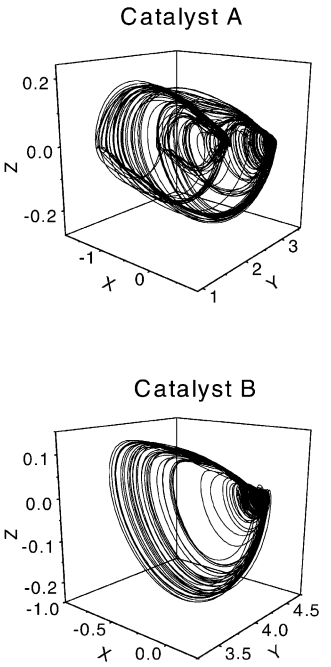

Fig. 8. Strange attractors, constructed by the differential method from the time series shown in Fig. 7a.

to reconstruct the system trajectory in d-dimensional phase space. Apparently, the most natural way to do this is by using integro-differential coordinates. For example, one could set

$$x_1(t) = \int_0^t (s(\tau) - \bar{s})\,\mathrm{d}\tau, \qquad x_2(t) = s(t),$$
$$x_3(t) = \dot{s}(t), \ldots, \tag{1}$$

where $\bar{s} = N^{-1}\sum_1^N s_k$ is the average value of s for the whole time series, and integrals and derivatives are calculated with the help of standard discrete approximations. Fig. 8 demonstrates the projection of the phase trajectory onto the subspace of the first three coordinates (1). The drawback of coordinates (1) is the increase of the noise/signal ratio with the increase of the order of the derivative. For this reason time delay coordinates instead of differential coordinates are often used in data processing of high-dimensional systems. Time delay coordinates with a time delay of 2 s were used for the evaluation of the maximal Lyapunov exponent below [22].

Fig. 8 shows the different structures of the strange attractors for both catalysts A and B. In the case of catalyst A containing 10 nm Pd particles the trajectories cover the attractor more homogeneously. The largest Lyapunov exponent was evaluated for each time series by the Rosenstein method and found to be 0.11 bit/s for catalyst A and 0.09 bit/s for catalyst B. These values indicate a larger exponential divergence of nearby trajectories on the attractor in the case of catalyst A and supports the conclusions which can be made from the visual inspection of the strange attractors shown in Fig. 8. The advantage of the Rosenstein method is that it allows to evaluate not only the largest Lyapunov coefficient but also the embedding dimension. The analysis of the time series shown in Fig. 8 revealed that for both attractors the embedding dimension is more than 10, i.e., in both cases we may deal with chaos in a high-dimensional phase space.

3.2. Coupling of local oscillators on the level of the catalyst bed

One of the proposed causes for the appearance of chaos during CO oxidation over Pd zeolite catalysts was the existence of various nonuniformities in the catalyst bed including a spatial variation of the Pd loading or catalyst density [23]. It was suggested further that due to these nonuniformities various parts of catalyst bed could display oscillations with different autonomous frequencies. The chaotic oscillations were supposed to originate if the global coupling through the gas phase did not lead to a full synchronisation.

To analyse the strength of coupling through the gas phase, the oxidation of CO has been studied over an inhomogeneous catalyst bed simulated by two adjacent catalyst layers on the same holder, the properties of which varied due to the different size of the palladium particles (see Fig. 2). The amount of the catalysts used was chosen such that the Pd surface area was the same for both catalysts. The oscillatory behaviour of each catalyst was monitored with the help of sensitive thermocouples on the surface. Each thermocouple responds to the heat production due to the reaction rate in the vicinity of its spotweld. To eliminate coupling through the gas phase a Teflon partition could be inserted in the reactor between the two catalysts as shown in Fig. 1 [24].

As a first step, the experiments had been carried out with the catalyst layer, combined from 30.2 mg of catalyst A and 12.2 mg of catalyst B, i.e., for a Pd surface area of 7.5 cm^2 for each of the catalysts. The conditions of the experiment corresponded to those, presented in Fig. 3, where the different natural

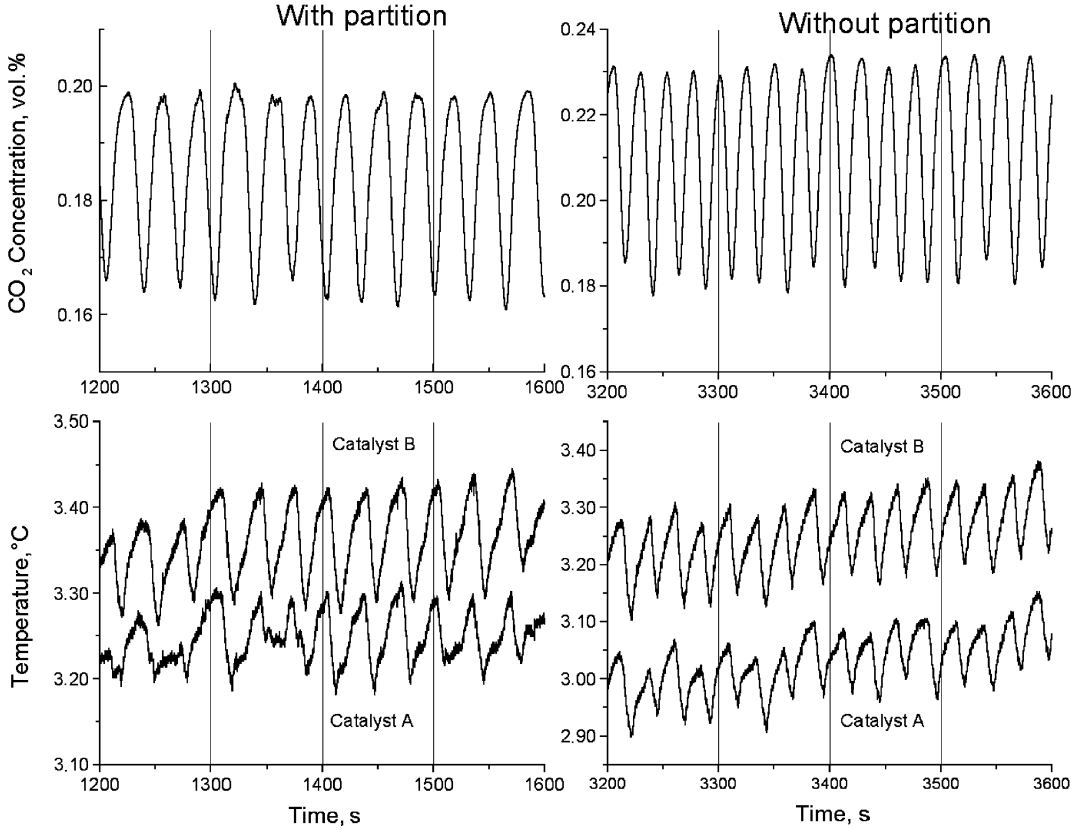

Fig. 9. The dynamic behaviour of catalysts A and B at 503 K and 0.5% CO inlet concentration without (left-hand side) and with (right-hand side) global coupling. Top: global reaction rate; bottom: temperature oscillations on the individual catalysts (from Ref. [24] reproduced by permission of the Royal Society of Chemistry).

frequencies of catalysts A and B were established in independent experiments. However, it has to be pointed out that the dynamical properties of the catalysts change with time on stream and while the properties of the oscillations can be reproduced in principle in repeated experiments identical time series cannot be expected.

Fig. 9 demonstrates the individual dynamic behaviour of catalysts A and B as monitored by the thermocouples and the global reaction rate at a CO inlet concentration of 0.5% in both cases, i.e., with and without separation of the reactor volume between the two catalyst beds. Surprisingly, even with the mass transfer through the gas phase impeded by the Teflon wall both catalysts oscillate with the same period and similar waveforms. Without partition, a fully synchronised behaviour can be observed (right-hand side of Fig. 9).

The largest difference between natural frequencies of reaction rate oscillations over zeolite catalysts containing various sizes of Pd particles was found for catalysts C and D containing only 0.01% Pd. The comparison of the natural frequencies of both catalysts at 503 K and 0.7% CO inlet concentration are shown in Fig. 10. The high conversion and the shape of the oscillations indicate that for the smaller Pd content, both catalysts seem to operate in a more reduced state in spite of their pre-treatment with oxygen. Fig. 11 depicts the properties of the individual oscillations of catalysts C and D and the global reaction rate at the same inlet CO concentration in the reactor with and without partition by the Teflon wall. To keep the Pd surface the same and equal to 1.25 cm^2, 25 mg of catalyst C was placed next to 10 mg of catalyst D (see Table 1). In the isolated case, catalysts C and D oscillate with different waveforms and with different natural periods of 68.2 and 51.2 s, respectively. The global reaction rate displays complicated oscillations with large peaks at moments, when the peak in the reaction rate happens to coincide for both catalysts. Without Teflon partition the temperature of both catalysts oscillates in phase indicating, that global coupling through the gas

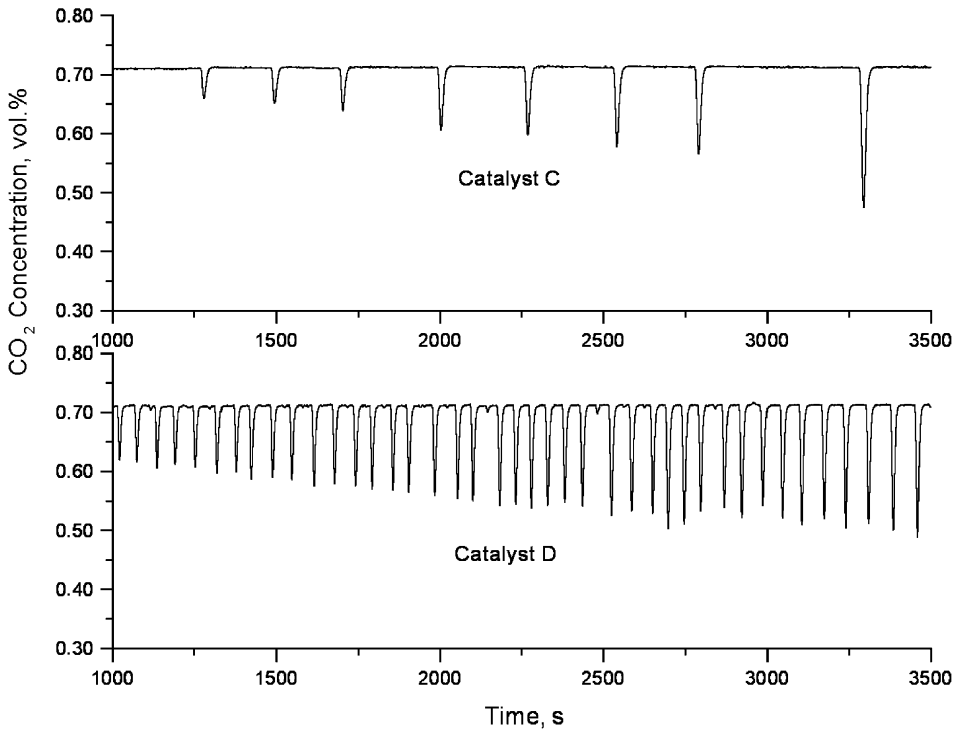

Fig. 10. Oscillatory behaviour of catalysts C and D at 503 K and 0.7% CO inlet concentration (from Ref. [24] reproduced by permission of the Royal Society of Chemistry).

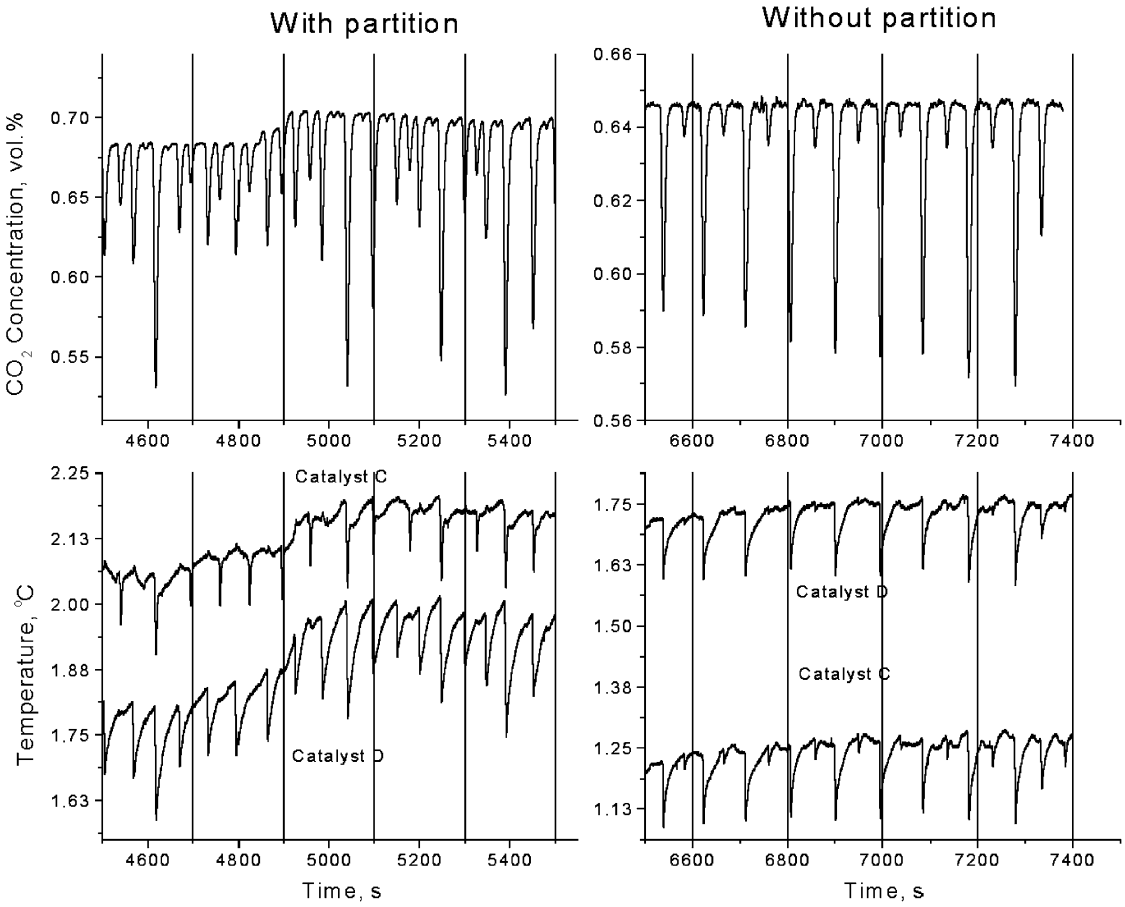

Fig. 11. The dynamic behaviour of catalysts C and D at 503 K and 0.7% CO inlet concentration without (left-hand side) and with (right-hand side) global coupling. Top: global reaction rate; bottom: temperature oscillations on the individual catalysts (from Ref. [24] reproduced by permission of the Royal Society of Chemistry).

phase is strong enough for the synchronisation of local oscillators with different natural frequencies. The analysis of the Fourier spectra demonstrated that even with the mass transfer through the gas phase impeded by the Teflon wall oscillations of the global reaction rate do not represent the superposition of natural frequencies of catalysts C and D. This experimental result indicates that some communication between the two catalyst beds exists even in the case of the Teflon partition, i.e., coupling must still exist to a certain extent either via heat transfer or via gas phase diffusion through the glass frit supporting the catalyst. Heat transfer could be ruled out in the case of the support of low heat conductivity. It can be also shown that an empty part of the frit does not show temperature oscillations in the neighbourhood of an oscillating catalyst bed. Therefore the gas phase coupling through the glass frit supporting the catalyst occurs and it may even be the dominant mechanism of synchronisation in the case of the partitioned reactor volume if the natural frequencies of both oscillators were close to each other as under the conditions shown in Fig. 9.

4. Discussion

The results presented demonstrate that regular periodic reaction rate oscillations over Pd zeolite catalysts

can only be observed in a very narrow interval of experimental conditions, i.e., for a pre-oxidised catalyst containing 10 nm Pd clusters and for low CO concentrations in the feed. Under most experimental conditions complex aperiodic and chaotic oscillations were detected.

The oxidation of CO over Pd zeolite catalysts can be considered as a complex multilevel heterogeneous catalytic system. Oscillatory behaviour may arise on the very first level, which is an element of a single crystal plane. The Pd cluster of 4 or 10 nm in diameter can be considered as the second level of the system followed by a zeolite crystallite of 5 μm in diameter, which is the analogue of a pellet of a common supported catalyst. It contains around 7×10^3 Pd clusters in the case of catalyst A and 10^5 Pd clusters in the case of catalyst B. The catalyst bed then consists of about 10^9 zeolite crystallites in the case of catalyst A and 10^8 zeolite crystallites in the case of catalyst B. The observation of regular periodic oscillations of the global reaction rate in a CSTR was indicative of complete synchronisation of local oscillators on all levels of the system such as the single nanometre-sized palladium cluster, the zeolite crystallite of micrometre size supporting many metal clusters and the catalyst bed consisting of many zeolite crystallites. In this case the properties of the regular oscillations may give information even about the catalytic processes which occur on a single palladium cluster.

4.1. Simulation of regular oscillations

Numerous studies of CO oxidation over Pd zeolite catalysts have established that the driving force for the appearance of kinetic oscillations in this system is the occurrence of a periodic oxidation and reduction of the Pd [15,16]. This mechanism has been supported by "in situ" X-ray absorption spectroscopy [17] and FTIR measurements of adsorbed CO [23]. The presence of the subsurface oxygen also explains the unusual counter-clockwise hysteresis in the reaction rate shown in Fig. 2.

The simplest mathematical model, describing the appearance of oscillations on the level of an element of a Pd surface was suggested in Ref. [25]. It was based on the Langmuir–Hinshelwood mechanism, which was modified to include the processes of the periodic formation and reduction of the subsurface oxygen:

$$\mathrm{CO} + \mathrm{M} \underset{k_{-1}}{\overset{k_1}{\Leftrightarrow}} \mathrm{MCO}, \qquad \mathrm{O_2} + 2\mathrm{M} \overset{k_2}{\Rightarrow} 2\mathrm{MO},$$

$$\mathrm{MCO} + \mathrm{MO} \overset{k_3}{\Rightarrow} \mathrm{CO_2} + 2\mathrm{M}, \quad \mathrm{MO} + \mathrm{M_v} \overset{k_4}{\Rightarrow} \mathrm{M_vO} + \mathrm{M},$$

$$\mathrm{M_vO} + \mathrm{MCO} \overset{k_5}{\Rightarrow} \mathrm{CO_2} + \mathrm{M_v} + \mathrm{M}, \tag{2}$$

where M denotes vacant sites on the metal surface, MCO and MO adsorbed CO and oxygen atoms, respectively. M_v indicates free sites and M_vO sites occupied by oxygen atoms in the subsurface layer.

The dynamic behaviour of the adsorbed species (x, y) and of the dissolved oxygen in the subsurface layer (z) can be described by the following equations:

$$\frac{\mathrm{d}x}{\mathrm{d}t} = k_1 P_{\mathrm{CO}}(1 - x - y) - k_{-1}x - k_3xy - k_5xz,$$

$$\frac{\mathrm{d}y}{\mathrm{d}t} = k_2 P_{\mathrm{O_2}}\, \mathrm{e}^{-\alpha z}(1 - x - y)^2 - k_3xy - k_4y(1 - z),$$

$$\frac{\mathrm{d}z}{\mathrm{d}t} = k_4y(1 - z) - k_5xz. \tag{3}$$

The main nonlinearity in the equations, which is responsible for the appearance of reaction rate oscillations is the exponential dependence of the oxygen adsorption rate upon the concentration of the subsurface oxygen. This feedback mechanism and the value of parameter $\alpha = 10$ was taken from the study of CO oxidation over a Pd(1 1 0) single crystal surface [26].

To simulate the dynamic behaviour of a homogeneous catalyst surface in a CSTR equation (5), which describes the variation of the CO partial pressure in the reactor must be added to Eq. (3):

$$\frac{\mathrm{d}P_{\mathrm{CO}}}{\mathrm{d}t} = \gamma(P^0_{\mathrm{CO}} - P_{\mathrm{CO}}) - \beta(k_1 P_{\mathrm{CO}}(1 - x - y) - k_{-1}x). \tag{4}$$

Here $\gamma = F/V_k$, $\beta = (N_s SRT)/V_k$, where F denotes the flow rate of the reactant mixture, V_k is the volume of the catalyst bed, S the Pd surface area, N_s the adsorption capacity of Pd. The values of these parameters correspond to the experimental conditions and are summarised in Table 2.

The simple model (3) can be used for the analysis of the main properties of oscillations, arising in this system due to periodic formation and reduction of the subsurface oxygen. In the high activity state the oxygen coverage is large, while the concentrations of

Table 2
Parameters of the experimental study used in the calculations

Flow rate, F	cm^3/s	2.5
Volume of the catalyst bed, V_k	cm^3	4.61×10^{-2}
Pd surface area, S	cm^2	15.1
The adsorption capacity, N	mol/cm^2	1.67×10^{-9}
R	cm^3 Torr/(mol grad)	6.15×10^4

adsorbed CO and of subsurface oxygen are relatively small. Under these conditions the adsorbed oxygen penetrates into the subsurface region and the concentration of the subsurface oxygen increases. At some point, the oxygen adsorption rapidly decreases and the surface is covered mainly by adsorbed CO. This is the low activity state. Thereafter a slow increase of the reaction rate occurs due to the reduction of the subsurface oxygen by adsorbed CO. When the critical concentration of the subsurface oxygen is passed, oxygen adsorption is facilitated and the high activity state will be reached again.

In dependence on the chosen parameters, model (3) together with Eq. (4) can describe various waveforms and periods of oscillations. Fig. 12a shows the relaxation oscillations with rate spikes "up". The waveform is typical for the low activity Pd zeolite catalysts just after the preliminary oxidation. The system spends more time in the low activity state with high CO coverage leading to the slow reduction of the subsurface oxygen. When a critical value is passed the system reaches the high activity state, in which the surface is mainly covered by oxygen. A rapid formation of subsurface oxygen causes the transition to the low activity state after a short time. A completely different waveform of oscillations with rate spikes "down" are demonstrated in Fig. 12b. Here the system spends more time in the high activity state, where the surface coverages are small, the concentration of adsorbed oxygen dominates and the formation of the subsurface oxygen proceeds relatively slow. The rate spike down then corresponds to the blocking of the surface by CO molecules at the critical concentration of the subsurface oxygen. At high CO coverage the reduction of the subsurface oxygen quickly proceeds and the system returns to the high activity state after a short time.

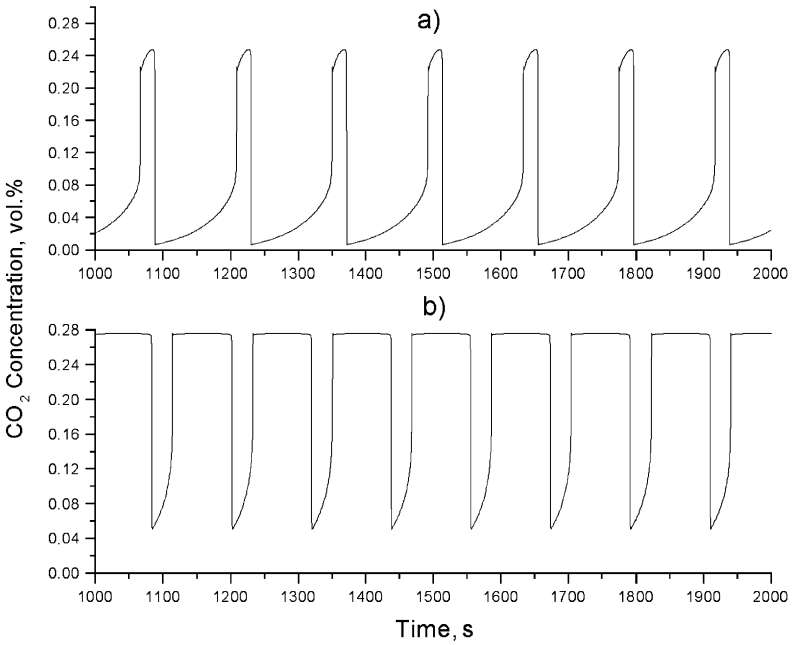

Fig. 12. Calculated reaction rate oscillations in a CSTR at $P_{O_2} = 160$ Torr and $P_{CO} = 2.16$ Torr, generated with mathematical model (4) for the following set of parameters: $k_1 = 120\,s^{-1}\,Torr^{-1}$, $k_2 = 92.5\,s^{-1}\,Torr^{-1}$, $k_4 = 0.0306\,s^{-1}$, $k_5 = 0.0042\,s^{-1}$. (a) Low activity oxidised catalyst, $k_{-1} = 13.95\,s^{-1}$, $k_3 = 50\,s^{-1}$; (b) reduced catalyst, $k_{-1} = 150\,s^{-1}$, $k_3 = 5000\,s^{-1}$.

Table 3
The values of the constants for the oxidised surface which were used in model (7)

	k_1	k_{-1}	k_2	k_3
k^0 (s^{-1} $Torr^{-1}$ or s^{-1})	120	6×10^9	250	4.35×10^7
E (cal/mol)	0	20000	1000	14000
k_i^1 (s^{-1} $Torr^{-1}$ or s^{-1})	120	13.93	92.5	39.32

The results of mathematical modelling shown in Fig. 12 demonstrate that oscillations with rate spikes down are produced by catalysts with the higher activity. The experimental observations are in excellent agreement with the results of the simulation, since such type of oscillations were observed over a Pd catalyst with higher activity which was reduced prior to the experiment. A similar variation of the shape of oscillations in dependence on the preliminary pre-treatment has been observed during the CO oxidation over polycrystalline platinum [27]. Solid electrolyte potentiometry (SEP) studies indicated that oscillations were caused by periodic formation and reduction of surface PtO_2. On the pre-oxidised low activity catalyst, the relaxation oscillations with rate spikes up were observed, while more active surface generated relaxation oscillations with rate spikes down. In case an oxidation–reduction mechanism operates for the system under investigation the analysis of the waveform of the oscillations may give information concerning the state of the active metallic component. From the analysis of the shape of the oscillations observed for catalysts A and B with various sizes of Pd clusters shown in Fig. 3, the conclusion can be drawn that 4 nm Pd clusters exist in a more reduced state compared to the 10 nm Pd clusters. The variation of the waveform and the period of regular oscillations with time (see Fig. 4) supports the hypothesis that a slow modification of the catalyst surface may take place due to the slow reduction of the catalyst A with 10 nm particles.

To model this process on an initially oxidised surface containing active centres of type M_1, the evolution of a new reduced surface is simulated by the appearance of new active sites of type M_2. According to the experimental observations, the initially oxidised surface M_1 does not produce oscillations and the steady state is achieved, corresponding to the ordinary Langmuir–Hinshelwood mechanism

$$\mathrm{CO} + [\mathrm{M_1}] \underset{k_{-1}^1}{\overset{k_1^1}{\Leftrightarrow}} [\mathrm{M_1{-}CO}], \quad \mathrm{O_2} + 2[\mathrm{M_1}] \overset{k_2^1}{\Rightarrow} 2[\mathrm{M_1{-}O}],$$

$$[\mathrm{M_1{-}CO}] + [\mathrm{M_1{-}O}] \overset{k_3^1}{\Rightarrow} \mathrm{CO_2} + 2[\mathrm{M_1}]. \qquad (5)$$

The rate constants of the reaction mechanism (5) listed in Table 3 were adjusted to obtain the steady-state value of the reaction rate over a pre-oxidised catalyst A. The experimental results depicted in Fig. 4 show that following the appearance of the oscillations amplitude and period slowly increase with time. This experimental fact was simulated by the formation of new active centres of type M_2 on the catalyst surface. These centres were responsible for the appearance of oscillations. It was supposed that the reaction over the reduced surface can produce oscillations due to the periodic formation and reduction of the subsurface oxygen

$$\mathrm{CO} + [\mathrm{M_2}] \underset{k_{-1}^2}{\overset{k_1^2}{\Leftrightarrow}} [\mathrm{M_2{-}CO}], \quad \mathrm{O_2} + 2[\mathrm{M_2}] \overset{k_2^2}{\Rightarrow} 2[\mathrm{M_2{-}O}],$$

$$[\mathrm{M_2{-}CO}] + [\mathrm{M_2{-}O}] \overset{k_3^2}{\Rightarrow} \mathrm{CO_2} + 2[\mathrm{M_2}],$$

$$[\mathrm{M_2{-}O}] + [\mathrm{M_v}] \overset{k_4}{\Rightarrow} [\mathrm{M_v{-}O}] + [\mathrm{M_2}],$$

$$[\mathrm{M_v{-}O}] + [\mathrm{M_2{-}CO}] \overset{k_5}{\Rightarrow} \mathrm{CO_2} + [\mathrm{M_v}] + [\mathrm{M_2}]. \qquad (6)$$

The constants of the reaction mechanism (6) were fitted to describe reaction rate oscillations over reduced surface. Table 4 gives a listing of all constants obtained for the reduced surface. It was also supposed that the oxidised surface with active centres M_1 can transfer to the reduced one with active centres M_2 and back via the following steps:

$$[\mathrm{M_1{-}CO}] \overset{k_6}{\Rightarrow} [\mathrm{M_2{-}CO}], \qquad [\mathrm{M_2{-}O}] \overset{k_7}{\Rightarrow} [\mathrm{M_1{-}O}].$$

Table 4
The values of the constants for the reduced surface which were used in model (7)

	k_1	k_{-1}	k_2	k_3	k_4	k_5
k^0 (s^{-1} $Torr^{-1}$ or s^{-1})	120	6.5×10^{10}	2.5×10^{2}	5.53×10^{8}	8.27×10^{-3}	8.88×10^{-1}
E (cal/mol)	0	20000	1000	14000	1000	10000
k_i^2 (s^{-1} $Torr^{-1}$ or s^{-1})	120	150	92.5	5000	0.0306	4.3×10^{-3}

The rate of the reduction step 6 is assumed to be proportional to CO coverage, while the rate of the oxidation step 7 is assumed to increase with the coverage of oxygen. The complete mathematical model can be written as follows:

$$\frac{dx_1}{dt} = k_{11}P_{CO}(\alpha - x_1 - y_1) - k_{-11}x_1 - \frac{k_{31}x_1y_1}{\alpha} - k_6x_1,$$

$$\frac{dy_1}{dt} = \frac{k_{21}P_{O_2}(\alpha - x_1 - y_1)^2}{\alpha} - \frac{k_{31}x_1y_1}{\alpha} + k_7y_2,$$

$$\frac{dx_2}{dt} = k_{12}P_{CO}(\beta - x_2 - y_2) - k_{-12}x_2 - \frac{k_{32}x_2y_2}{\beta} - \frac{k_5x_2z_2}{\beta} + k_6x_1,$$

$$\frac{dy_2}{dt} = \frac{k_{22}P_{O_2}\,e^{-\alpha z_2/\beta}(\beta - x_2 - y_2)^2}{\beta} - \frac{k_{32}x_2y_2}{\beta} - \frac{k_4y_2(\beta - z_2)}{\beta} - k_7y_2,$$

$$\frac{dz_2}{dt} = \frac{k_4y_2(\beta - z_2)}{\beta} - \frac{k_5x_2z_2}{\beta},$$

$$\frac{d\beta}{dt} = k_6x_1 - k_7y_2,$$

$$\frac{dP_{CO}}{dt} = \frac{F}{V_r}(P_{CO}^0 - P_{CO}) - \frac{SNRT}{V_r}((k_{11}P_{CO}(\alpha - x_1 - y_1) - k_{-11}x_1) + (k_{12}P_{CO}(\beta - x_2 - y_2) - k_{-12}x_2)), \quad (7)$$

where α is the part of the surface with active centres M_1, while β the part of the whole surface with active centres M_2 ($\alpha + \beta = 1$)

Fig. 13 demonstrates the result of the simulations obtained with model (7) and parameters presented in Tables 2–4. All the experimental trends are reproduced by model (7) including the values of period and amplitude and their growth with time. The value of β in time slowly increases indicating the larger amount of the reduced surface, where oscillations can develop. Their amplitude and period become larger with the increase of β. The simulation reproduces also the experimental observation that with the development of oscillations the system spends more time in the high activity state.

4.2. The origin of chaos in the system

The experimental data demonstrate that chaotic oscillations are observed under most experimental conditions. The increase of the activity due to the reduction of the catalyst, the increase of the temperature of the catalyst and of the CO concentration in the feed favour the appearance of chaotic oscillations. Two additional important parameters are the size of the supporting zeolite crystallite and the size of Pd clusters. It was shown in the experiments that the decrease of the size of the Pd clusters creates more favourable conditions for the appearance of chaotic behaviour. Earlier it was demonstrated that for a constant size of the Pd clusters (10 nm) and under the same experimental conditions regular periodic oscillations were observed in the case of 5 μm and chaotic behaviour in the case of 50 μm supporting zeolite crystallites, respectively [16].

Prior to the mathematical modelling of chaotic oscillations it is necessary to identify the level on which a heterogeneous catalytic system generates chaotic oscillations. The high embedding dimensions of the strange attractors shown in Fig. 8 indicate that chaotic behaviour does not appear on the first level, namely for the Pd single crystal surface, where the dynamic behaviour is described by a point or lumped mathematical model. As a rule such models generate low-dimensional chaos in a very narrow range of model parameters. Most likely, the experimen-

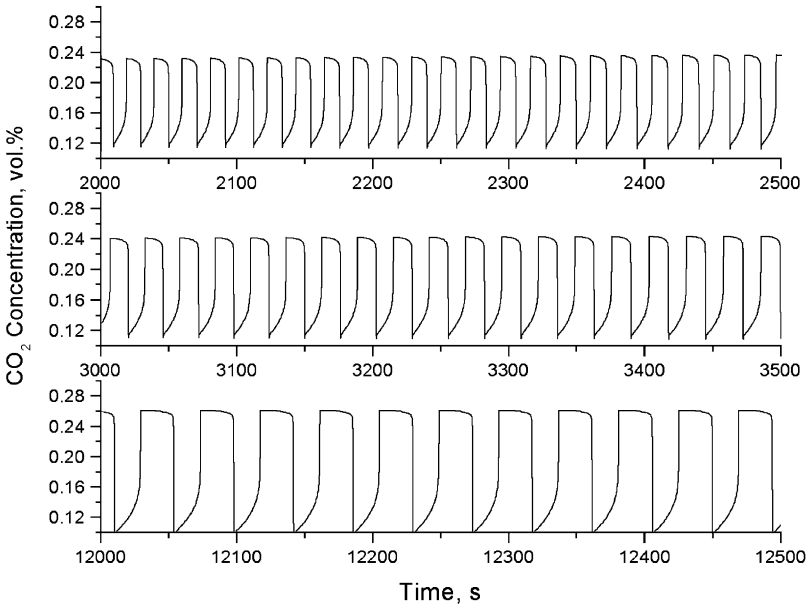

Fig. 13. The development of the regular oscillations generated by model (7) with parameters from Tables 2–4 with $k_6 = 0.007\,s^{-1}$ and $k_7 = 0.001\,s^{-1}$.

tally observed chaotic behaviour represents a chaos in a high-dimensional space, which mainly arises in distributed systems such as arrays of coupled local oscillators. Experimental data presented in Section 3 allow us to exclude the appearance of chaotic oscillations due to insufficient synchronisation of various inhomogeneous parts of the catalyst layer as one of the origins of chaotic behaviour. The obtained results clearly demonstrate that in the system under investigation global coupling through the gas phase is so strong that even various catalysts producing different natural frequencies can easily be synchronised. If the difference in the natural frequencies is not too large various catalysts produce synchronous behaviour even in the reactor with partition, where the gas phase coupling through the porous support appears to be sufficient for the synchronisation.

Presumably, the chaotic behaviour originates on the level of a zeolite crystallite. The results of the simulations presented in Ref. [28] demonstrated that the increase of the gradient of the CO concentration within the zeolite crystallite may cause the breakdown of the synchronisation of Pd clusters situated at various distances from the centre of the zeolite crystallite and cause the chaotic behaviour. This is the case of the so-called "diffusional chaos" in distributed systems. However, using the oversimplified point model (3), which does not consider the variation of the state of Pd with CO partial pressure, chaotic behaviour was obtained only in a very narrow region of parameters and for a value of the constant for CO diffusion within the zeolite crystallite larger than experimentally established [29]. The improvement of the point model, namely by the variation of the state of the Pd in dependence on the CO partial pressure may produce chaotic oscillations in a much larger region of the parameter space and closer to more realistic experimental conditions. Modelling of these effects is currently in progress for the present system.

5. Conclusions

Zeolite supported palladium catalysts are suitable model systems for the study of the influence of experimental parameters like the size of the palladium clusters and reactant concentrations on the oscillatory behaviour of the catalytic system. The synchronisation

of local oscillators is required to establish global reaction rate oscillations on various levels of a catalytic system. For the oscillating catalytic oxidation of CO on zeolite supported palladium catalysts, global coupling through mass transport in the gas phase could be established as the dominant mechanism on the level of the catalyst bed in a CSTR. Heat transfer can be the dominant coupling mechanism in the case of a support of high heat conductivity.

The size of the palladium clusters embedded within the zeolite matrix shows a strong influence on the structure of the observed reaction rate oscillations. Simulations show that characteristic features like the activity of the catalyst as well as period and amplitude of the oscillations can be captured by adding a variation of the state of the oxidation of the palladium clusters to a common kinetic model.

The analysis of aperiodic time series yields chaotic attractors in a phase space of high dimension indicative of diffusional chaos that is characteristic for distributed systems.

Acknowledgements

The authors acknowledge financial support from INTAS (grant 99-1882), the Russian Fund of Fundamental Researches (grant 00-03-32125) and from the VolkswagenStiftung (I70/600).

References

[1] F. Schüth, B.E. Henry, L.D. Schmidt, Adv. Catal. 39 (1993) 51.
[2] M.M. Slinko, N.I. Jaeger, Oscillating heterogeneous catalytic systems, Studies in Surface Science and Catalysis, Vol. 86, Elsevier, Amsterdam, 1994.
[3] R. Imbihl, G. Ertl, Chem. Rev. 95 (1995) 697.
[4] G. Ertl, Adv. Catal. 37 (1990) 213.
[5] R. Imbihl, in: P.J. Plath (Ed.), Springer Series in Synergetics, Vol. 44, Springer, Berlin, 1989, p. 26.
[6] P.K. Tsai, M.B. Maple, R.K. Herz, J. Catal. 113 (1988) 453.
[7] H.U. Onken, E.E. Wolf, Chem. Eng. Sci. 43 (1988) 2251.
[8] M. Eiswirth, in: R.J. Field, L. Gyorgyi (Eds.), Chaos in Chemistry and Biochemistry, World Scientific, Singapore, 1993.
[9] M.C. Cross, P.C. Hohenberg, Rev. Mod. Phys. 65 (1993) 851.
[10] M. Eiswirth, K. Krischer, G. Ertl, Surf. Sci. 202 (1988) 565.
[11] P.D. Cobden, J. Siera, B.E. Nieuwenhuys, J. Vac. Sci. Technol. A 10 (1992) 2487.
[12] G. Veser, R. Imbihl, J. Chem. Phys. 100 (1994) 8492.
[13] L.F. Razon, S.-M. Chang, R.A. Schmitz, Chem. Eng. Sci. 41 (1986) 1561.
[14] H.U. Onken, E. Wicke, Ber. Bunsen-Ges. Phys. Chem. 90 (1986) 976.
[15] M.M. Slinko, N.I. Jaeger, P. Svensson, J. Catal. 118 (1989) 349.
[16] N.I. Jaeger, M.A. Liauw, P.J. Plath, J. Chem. Phys. 104 (1996) 6375.
[17] Th. Ressler, M. Hagelstein, U. Hatje, W. Metz, J. Phys. Chem. B 101 (1997) 6680.
[18] L. Drozdova, J. Novakova, G. Schulz-Ekloff, N.I. Jaeger, Microporous Mesoporous Mater. 28 (1999) 395.
[19] G. Schulz-Ekloff, in: J.L. Atwood, J.E.B. Davies, D.D. Macnicol, E. Vögtle (Eds.), Comprehensive Supramolecular Chemistry, Vol. 7, Pergamon Press, Oxford, 1996, p. 549.
[20] M.T. Rosenstein, J.J. Collins, C.J. DeLuca, Physica D 65 (1993) 117.
[21] H.G. Schuster, Deterministic Chaos, 2nd Revised Edition, VCH, Weinheim, 1988.
[22] M.M. Slinko, A.A. Ukharskii, N.V. Peskov, N.I. Jaeger, Faraday Discuss. 120 (2001), in press.
[23] M.A. Liauw, Dissertation, University of Bremen, 1994.
[24] M.M. Slinko, A.A. Ukharskii, N.I. Jaeger, Phys. Chem. Chem. Phys. 3 (2001) 1015.
[25] M.M. Slinko, E.S. Kurkina, M. Liauw, N. Jaeger, J. Chem. Phys. 111 (1999) 8105.
[26] M.R. Basset, R. Imbihl, J. Chem. Phys. 93 (1990) 811.
[27] I.V. Yentekakis, S. Neophytides, C.G. Vayenas, J. Catal. 111 (1988) 152.
[28] E.S. Kurkina, N.V. Peskov, M.M. Slinko, Physica D 118 (1998) 103.
[29] J. Kärger, H. Pfeifer, F. Stallmach, N.N. Feoktistova, S.P. Zhdanov, Zeolites 13 (1993) 50.